Earthquake Engineering, Tenth World Conference © 1992 Balkema, Rotterdam ISBN 90 5410 060 5

Dynamics and dispersion mechanism in a four span bridge

S. Kitagawa, K. Uno & T. Aso
Department of Civil Engineering, Kyushu University, Fukuoka, Japan

T. Yasumatsu
Japan Highway Public Corporation, Fukuoka, Japan

ABSTRACT: Bridges with rubber bearings have been constructed with a mechanism of dispersing the horizontal reactive forces. Free vibration test and microtremor measurements were conducted on a four span continuous PC bridge with rubber bearings. Eigenvalue analysis with finite element method and Response analysis with spectrum method were carried out to investigate the dynamic characteristics of the bridge. The effectiveness of the rubber bearings as an earthquake resistant device is verified by the results of the experiment and analysis.

1 INTRODUCTION

Recently, rubber bearings have been introduced in prestressed concrete (PC) bridges to disperse the horizontal forces. This form of supporting the super-structure provides a stable restraint against shrinkage and creep, temperature stresses and inertial effects of the earthquake, by dispersing the horizontal reactive forces at the bearing level. So far, though a few similar bridges have been constructed, Shimizugawa bridge is the rare such example to verify the dynamic characteristics of this kind of structure. Experiments were conducted on this bridge with oil pressure actuator to determine static load-displacement relationship and it free vibration characteristics. In this bridge, the inertial force of the top slab is divided and dispersed horizontally by special dispersion mechanisms. Presently, the earthquake resistant design standardization for such structures is inadequate. Here, we carried out the dynamic analysis and an evaluation of its dynamic characteristics.

2 EXPERIMENTS

This bridge consists of four span continuous PC box girders and a PC T-girder span with a total bridge length of 295m as shown in Figure 1. The sliding ring shoes are used on the P8 and P12 piers and reaction force dispersion shoes on P9~P11. Two oil pressure jacks (of maximum capacity:180t, and displacement limit:150mm) with a valve that can be opened rapidly; owned by the public corporation, were set on each pier from P9 to P11 as loading devices. The shearing deformation of each rubber shoe and absolute displacement of the girder at P12 and A2 were measured.

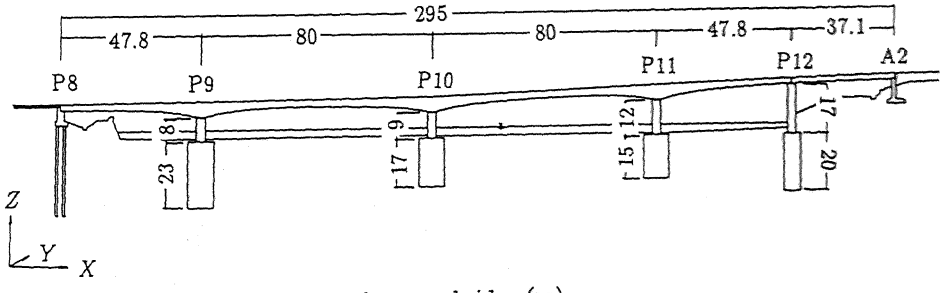

Fig.1 Longitudinal section of Simizugawa bridge (m)

2.1 Horizontal loading test for each pier

A horizontal loading of 300ton or less was applied at each pier to find the rigidity of the pier and the soil spring constant. Figure 2 shows the relation between the relative displacement of rubber shoes and the load on P9, P10 and P11. Figure 3 shows shear spring constants of the rubber bearings from performance tests. The shared force at each pier and the frictional force of sliding ring shoes was calculated by the amount of shearing deformation of rubber shoes obtained from the experiments. This frictional force at the sliding ring shoes is assumed to be equal, as these shoes are of the same type. The results are shown in Table 1. Soil spring constant(K) was calculated by the relation between the horizontal force and displacement at the pier, and used for the eigenvalue analysis.

2.2 Horizontal simultaneous loading test for 3 piers

Horizontal loading was applied at the same time until the displacement at each pier reached 40mm or less to find the shared force of each pier. Figure 4 shows the relation between the absolute displacement of girder and the load on P9, P10 and P11. The relation between the shared forces and the load, until when the load was increased gradually is shown in Figure 5. The difference between all loads and the sum of all shared forces is the frictional force at the sliding ring shoes. The shearing spring constant indicates a bilinear characteristics as in Figure 3, and all shared force is somewhat different in the experimental and the design value.

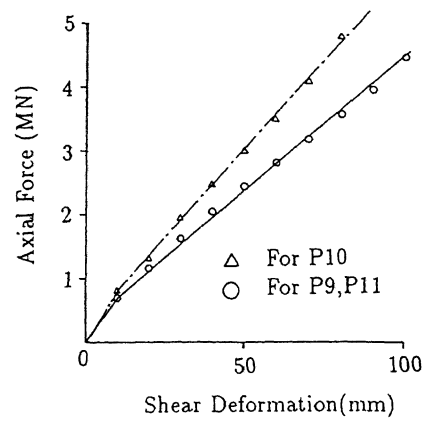

Fig.3 Shear spring constant

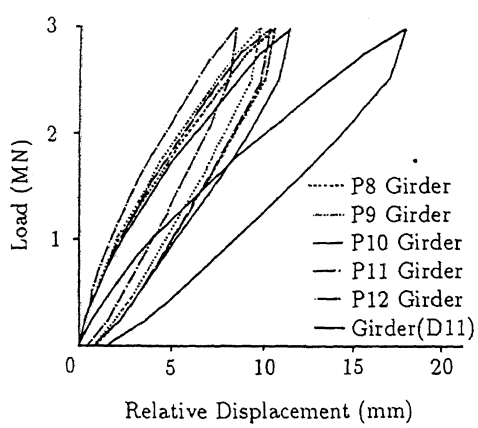

Fig.2 Pier load vs shear deformation

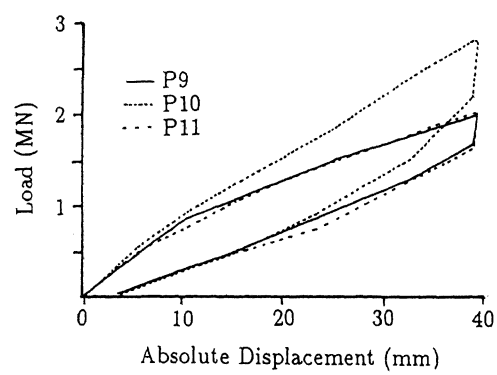

Fig.4 Pier load vs displacement of pier

Table 1. Shared force and frictional force

Loaded Pier	Load F (kN)	Shared Force (kN) Q8	Q9	Q10	Q11	Q12	Top of Pier S (kN)	Disp. (mm)
P9	2450	274	862	539	500	274	1588	5.37
P10	2930	196	696	1225	617	196	1705	6.17
P11	2930	137	725	745	1186	137	1744	8.94

F = Q8+Q9+Q10+Q11+Q12
S = F - Qn (n=9,10,11)

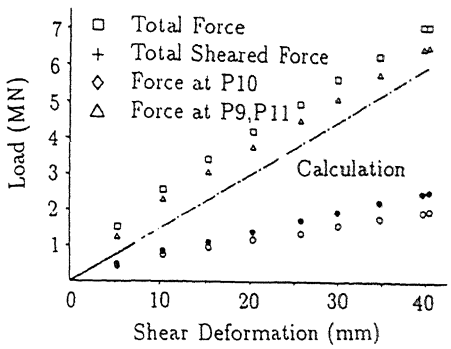

Fig.5 Pier load vs shear deformation

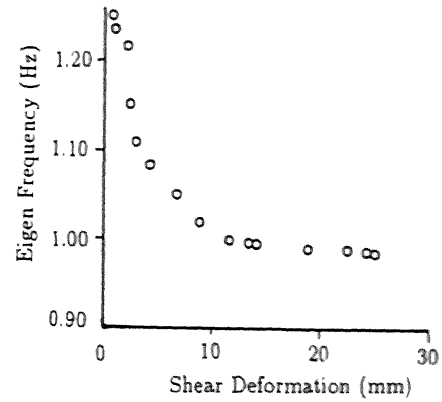

Fig.6 Eigen frequency vs shear deformation

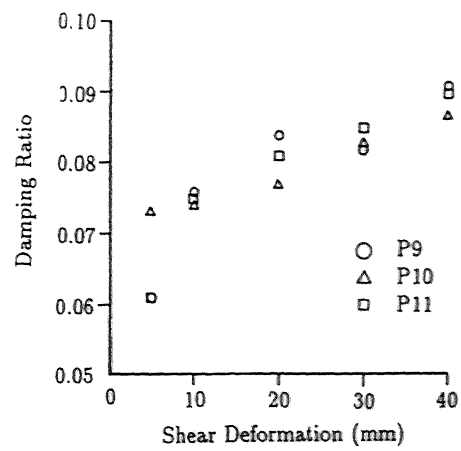

Fig.7 Damping ratio vs shear deformation

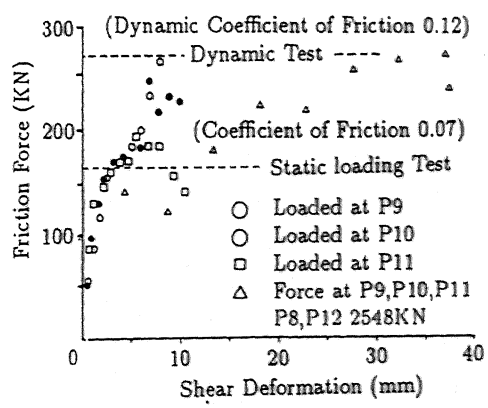

Fig.8 Sliding(Rubber bearing) shoe deformation

2.3 Free vibration test

The horizontal load was applied until the horizontal displacement reached 30mm as well as §2.2, the jack pressure was suddenly released and the free vibration test of the girder and the pier was carried out. The first natural frequency and the damping coefficient were determined by this test (Figure 6,7). The damping coefficient increases with increase in the shearing deformation of the rubber shoes. This in comparison with ordinary bearings is considerably larger. On the other hand, the 1st mode i.e. longitudinal vibration frequency was decreasing with increase in the shearing deformation and is indirectly due to the frictional force at the sliding shoes. Figure 8 shows the relationship between the deformation and the frictional force at the piers. The frictional force tends to be constant beyond a 10mm displacement, indicating beginning of sliding. Figure 3 shows the stiffness variation beyond 10mm from the experiment, which is found to match values calculated from the friction force-deformation plot. It is expected that during strong earthquake motions resulting in a large ring shoe deformation, the natural frequency will be on the lower range of 0.9~1.1Hz. The first longitudinal mode was dynamically measured using oil pressure actuator whereas, other modes were extracted from the microtremor measurements. Especially all higher out of plane modes and vertical vibration modes were evaluated from the ambient vibration testing. Figure 9 shows the Fourier spectra for out of plane and vertical directions.

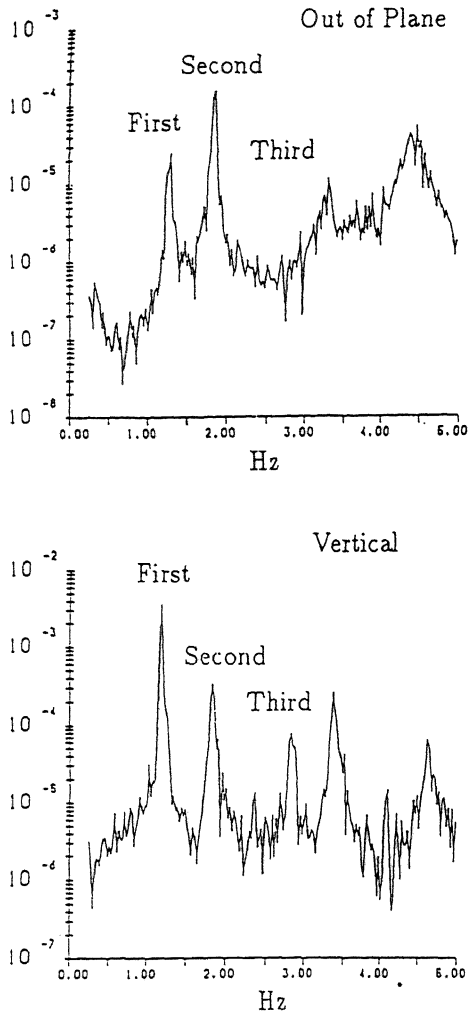

Fig.9 Fourier spectra

3 ANALYSIS

3.1 Eigenvalue analysis

A 128 nodes and 122 beam elements mathematical model was formulated and analyzed by a 3D-FEM analysis. The soil spring constant of the pier caisson was determined from a static load displacement test. This was necessitated because of large pier deformation during the out of plane modes and hence the large influence of soil stiffness on modal property. The mathematical model boundary conditions were modified to accommodate rubber shoes and sliding ring shoes at pier P8~P12. This was divided into 3 cases, such as

CASE I: the rubber bearings and the sliding ring shoes as shearing springs

CASE II: the rubber bearings as shearing springs and the sliding ring shoes as roller

CASE III: the rubber bearings as hinge and the sliding ring shoes as roller

CASE I corresponds to the case when the displacement of the girder is small and no sliding is detected and ring shoes behave as rubber bearings in the longitudinal 1st mode. In CASE II it is assumed that ring shoes slide responding to earthquake motions. For a comparison between rubber bearings and steel shoes, CASE III simulates the case, when rubber bearings is changed to the hinge. Table 2 shows the natural frequencies compared with the results obtained from experiments. Some displacement modes in CASE II are shown compared with the results of microtremor measurements in Figure 10. Figure 11 shows some modes in CASE III to be considerably different from CASE II. Comparing CASE II and III with the results of experiments in Table 2, the 1st mode corresponds to the longitudinal vibration in the free vibra-

Table 2. Eigen frequency (Hz)

MODE	Direction	CASE I	CASE II	CASE III	Vibration Test	Microtremor
1	$X-1$	0.81	0.75	–	0.92 ~ 1.10	–
2	$Z-1$	1.21	1.21	1.24	–	1.17
3	$Y-1$	1.57	1.57	1.64	–	1.29
*	X	–	–	1.67	–	–
4	$Y-2$	1.78	1.78	1.90	–	1.88
5	$Z-2$	1.89	1.89	1.93	–	1.83
6	$Y-3$	2.40	2.38	2.57	–	2.54
7	$Z-3$	2.95	2.96	2.96	–	2.83

X:Longitudinal, Y:Out of Plane, Z:Vertical

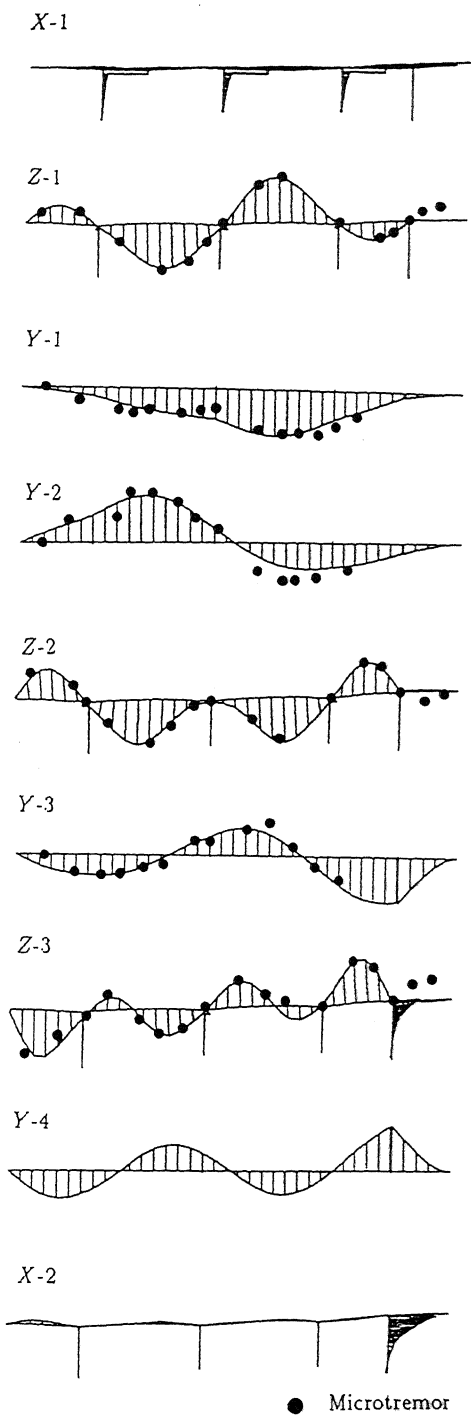

Fig.10 Displacement modes in CASE II

tion tests. On the other hand this mode was not detected during ambient vibration measurements. But the results from microtremor mea-

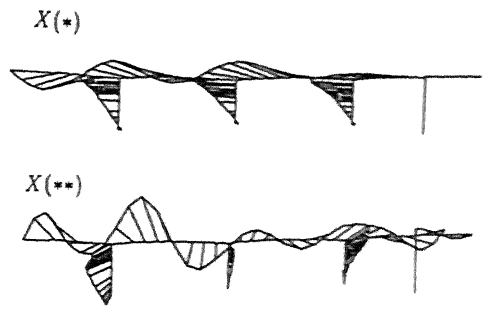

Fig.11 Displacement modes in CASE III

surements and the calculated values are almost comparable for higher modes. The eigen frequency of longitudinal 1st mode(*) in CASE III is about twice as much as in CASE II, which is the remarkable difference between CASE II and III. In CASE II, the girder only moves by the shear deformation of the rubber bearings, but in CASE III the whole girder and piers move as a single body in the longitudinal direction. As a result, the mode involving pier movement associated with the longitudinal motion of the girder has a higher eigen frequency in CASE II. In CASE III where the ring shoe was modeled as a roller, the P8, P12 piers vibrate in an independent modal shape, whereas, in other modes the whole moves as a single body. For inplane vibration, the CASE III eigen frequencies when compared to CASE II are a little bit higher. But the out of plane mode in Figure 10 shows that the pier moves significantly, requiring the addition of soil spring constant in the calculations.

3.2 Response characteristics of the bridge with rubber bearings

The CASE II results are comparable with the experimentally observed values. This fact shows the validity of the mathematical model in CASE II. The response calculations were carried using the response spectrum method and a long period excitation of the Hachinohe earthquake record, with a peak acceleration of 170gal.

Damping constant for all modes is 0.02, except the longitudinal 1st mode, which is 0.09 estimated from the free vibration test (maximum vibration displacement 16mm). Only the first 20 modes less below 5Hz frequency were used. The direction of input earthquake wave is horizontal (longitudinal and out of plane) and vertical. Vertical vibration is generally less than half of the horizontal vibration, so half of the peak val-

Table 3. Maximum value of response

	Direction	CASE II					CASE III				
		Girder	P9	P10	P11	P12	Girder	P9	P10	P11	P12
Disp. (cm)	X	14.4	1.8	2.5	2.7	2.1	5.9	5.2	5.4	5.8	2.8
	Y	10.7	1.9	6.0	5.6	1.9	9.6	2.0	5.9	5.6	2.3
	Z	1.2	0.2	0.1	0.1	0.1	1.2	0.2	0.1	0.1	0.1
Accel. (gal)	X	321	439	381	484	753	654	577	598	645	967
	Y	1060	256	608	574	402	1040	297	646	625	400
	Z	400	96	81	44	66	413	95	109	102	71
Bending Moment (MN·m)	R_Y (X)	12.6	43.4	58.5	61.6	19.1	36.0	103.9	121.5	130.3	250.8
	R_X (Y)	14.0	61.2	180.3	167.6	17.1	12.2	59.4	172.5	170.5	12.2
	R_Z (Y)	91.1	0.11	0.18	0.22	1.45	82.4	19.3	20.1	28.4	6.31

R_X:Inplane, R_Y:Out of Plane, R_Z:Inplane

ues of response spectrum in horizontal direction is used for that of vertical direction.

Table 3 shows results of earthquake response analysis. The values in Table 3 are maximum values of the girder and each pier P9, P10, P11, P12. When CASE II is compared with CASE III, the girder in the longitudinal inplane modes has a large displacement and a small response acceleration. However, for pier response the response acceleration and displacement are smaller in CASE II. This is reasoned in Figure 10 and 11. The out of plane response displacement and acceleration are comparable in both cases. The vertical excitation is taken as 1/2 of horizontal excitation. Due to the above reason the response values were smaller than the horizontally excited results.

The response moments for the inplane motion (R_Y) and torsional mode (R_Z) are smaller for CASE II when compared with CASE III. This shows that the use of rubber bearing results in a reduction of the pier bending moment, proving its effectiveness.

4 CONCLUSIONS

The static and dynamic test results of this bridge confirm the special utility and lateral load sharing characteristics. The rubber bearings produce rigid body mode dispersing the reactive forces and is indicative of these results. The dispersion of reactive forces through the use of rubber bearings causes the 1st mode to be the principal mode, and the reactive forces are substantially reduced. However, areas where long period motion is predominant, the longitudinal displacement can be fairly large enough to warrant the incorporation of additional displacement control mechanisms.

REFERENCES

Suzuki, Y. & Morita, N. 1990. Design, construction and vibration test of Ishikarigawa Bridge (Do-oh Highway). Prestressed Concrete. Vol.32, No.2:19-28.

Kiyota, R., Natori, T., Sasaki, Y. & Yoko-o, M. 1990. Vibration characteristics in five span continuous steel bridge with rubber bearings. Yokogawa Bridge Giho. No.19:21-36.

Matsuno, Y., Yoshida, K. & Muraoka, K. 1990. Design and construction of Shimizugawa Bridge at Kokubu-Hayato Road. Bridge Engineering.3 :32-41.

Yara,A., Nakasone,A., Toma,K. & Okado,M. 1989. Design and construction of Ikema Bridge. Bridge and Foundation Engineering.10:2-8.

Sakai, H., Sekiguchi, T. & Murao, Y. 1990. Design of PC continuous box girder bridge with fixed ends and rubber bearings based piers. Bridge Engineering.5:21-26.